

Fig. 3 Comparison of instantaneous velocity vectors in different spanwise planes of the swept wing at an incidence of 28 deg.

the top of the wing. Because the flow stays attached longer as z increases from -5 to $+5$ cm (-2 to $+2$ in.), the vorticity associated with the leading-edge shear layer continues to increase for a longer period of time at higher values of z . Therefore, one can expect the maximum lift to be higher and occur later as z increases. Indeed, the sectional lift data obtained in different spanwise planes in Ref. 3 indicated this behavior.

In the present setup, the distance of the pitch axis from the leading edge varies from $0.208c$ at $z = -5$ cm (-2 in.) to $0.25c$ at $z = 0$ to $0.292c$ at $z = +5$ cm ($+2$ in.). The progressive delay in stall and increase in maximum lift with increasing value of z are somewhat similar to those produced by a similar aftward shift in pitch-axis location in two-dimensional flows. However, the effects observed in the present studies are not merely quasi-two-dimensional. The progressive time delay of events across the wing span effectively causes the DSV front to propagate obliquely (from bottom left toward top right in the present case) over the wing surface as the angle of incidence increases. This explains the gradual washing away of the vorticity (as opposed to its rapid ejection from the surface), thereby preventing a catastrophic loss of overall lift. Flow visualization studies also confirmed the spreading of the stall over the wing surface in this manner.

Although the exact direction of spreading of the DSV and quantitative details associated with it depend on the pitch-axis geometry, the qualitative features of the DSV kinematics such as oblique spreading over the wing surface and gradual washing away of vorticity (leading to a gradual dynamic stall process) resemble the process of open-type separation often observed in steady three-dimensional flows.⁵ Hence, the qualitative features of dynamic stall observed in the present studies are probably generic to three-dimensional unsteady flows over all pitching wings.

Acknowledgment

The authors gratefully acknowledge support of this work by the U.S. Air Force Office of Scientific Research through Grant F49620-92-J-0146.

References

- ¹Conger, R. N., and Ramaprian, B. R., "Pressure Measurements on a Pitching Airfoil in a Water Channel," *AIAA Journal*, Vol. 32, No. 1, 1994, pp. 108–115.
- ²Oshima, H., and Ramaprian, B. R., "Velocity Measurements over a Pitching Airfoil," *AIAA Journal*, Vol. 35, No. 1, 1997, pp. 119–126.
- ³Patterson, A. K., Rymarz, P. B., and Ramaprian, B. R., "Surface Pressure Measurements on a Pitching Swept Wing in a Water Channel," *AIAA Journal*, Vol. 33, No. 10, 1995, pp. 1871–1879.
- ⁴Rymarz, P. B., "Measurements of Velocity and Vorticity Fields Around a Pitching Swept Wing," M.S. Thesis, Mechanical and Materials Engineering Dept., Washington State Univ., Pullman, WA, May 1995.
- ⁵Wang, K. C., "Separation Patterns of Boundary Layer over an Inclined Body of Revolution," *AIAA Journal*, Vol. 10, No. 8, 1972, pp. 1044–1050.

Boundary-Layer Characterization on Moving Walls by an Embedded Laser Velocimetry Technique

M. Pascazio,* J. M. Autric,* D. Favier,[†]
and C. Maresca[†]

Universités d'Aix-Marseille 1 et 2,
13288 Marseille Cedex 09, France

Nomenclature

c	= chord of the model, m
f	= frequency of oscillation, Hz
H	= integral shape factor, $H = \delta_1/\delta_2$
k	= reduced frequency of oscillation, $c\omega/2U_\infty$
Re	= Reynolds number, $U_\infty c/\nu$
Re_s	= local Reynolds number, $U_e(s, t)s/\nu$
s	= curvilinear distance along the wall from the leading edge, m
t	= time, s
U	= mean velocity tangent to the wall, ms^{-1}
U_e	= mean local external velocity, ms^{-1}
U_∞	= freestream velocity, ms^{-1}
u	= instantaneous tangent velocity (parallel to the wall), ms^{-1}
u'	= fluctuating tangent velocity, ms^{-1}
V	= mean velocity normal to the wall, ms^{-1}
v	= instantaneous velocity normal to the wall, ms^{-1}
y	= distance normal to the model wall, m
α	= instantaneous incidence of the model, deg
α_0	= mean incidence of the model, deg
δ	= boundary-layer thickness, m
δ_1	= integral displacement thickness, m
δ_2	= integral momentum thickness, m
δ_3	= first integral energy thickness, m
δ'_3	= second integral energy thickness, m
ν	= kinematic viscosity, m^2s^{-1}
σ_u	= tangential turbulence intensity, $\sigma_u = \sqrt{\langle u'^2 \rangle}/U_e$
ω	= angular frequency, $2\pi f$, rads^{-1}
ωt	= phase of the period, deg

Presented as Paper 96-0035 at the AIAA 34th Aerospace Sciences Meeting, Reno, NV, Jan. 15–18, 1996; received Feb. 5, 1996; revision received Sept. 18, 1996; accepted for publication Sept. 29, 1996; also published in *AIAA Journal on Disc*, Volume 2, Number 2. Copyright © 1996 by the American Institute of Aeronautics and Astronautics, Inc. All rights reserved.

*Graduate Student, Institut de Recherche sur les Phénomènes hors Équilibre/Laboratoire Aérodynamique Subsonique Institutionnaire, Unité Mixte de Recherche 138, Centre National de la Recherche Scientifique, 163, Avenue de Luminy, Case 918.

[†]Senior Research Scientist, Institut de Recherche sur les Phénomènes hors Équilibre/Laboratoire Aérodynamique Subsonique Institutionnaire, Unité Mixte de Recherche 138, Centre National de la Recherche Scientifique, 163, Avenue de Luminy, Case 918. Member AIAA.

Introduction

THE accurate determination of the boundary-layer response to unsteadiness produced by the forced motion of an airfoil requires additional investigations on basic unsteady flow phenomena, including unsteady transition, separation, reattachment, and laminarization processes that play a major role in aeronautical applications. In this Note, an embedded laser velocimetry measurement (ELV) method, suited for unsteady boundary-layer measurements on oscillating airfoils of arbitrary shape, has been developed. This method, based on an ELV optical fiber option, is an extension of a previous one tested on a one-dimensional longitudinal velocity field measured over an oscillating flat-plate model.^{1,2}

The present extension of the ELV method includes determination of the two-dimensional instantaneous velocity components (u , v),^{3,4} tangent and normal to the local wall curvature and the tangential turbulence intensity σ_u .

More specifically, transition and separation/reattachment phenomena of the boundary layer on a NACA 0012 airfoil oscillating in pitching motion [instantaneous incidence, $\alpha(t) = \alpha_0 + \Delta\alpha \cos \omega t$], at a fixed Reynolds number $Re = 10^5$, are studied from velocity component profiles. Steady and unsteady measurements of u , v , and σ_u have been performed at different distances from the leading edge of a NACA 0012 airfoil and for various conditions of k , α_0 . In particular, the U , V mean velocity profiles and σ_u profiles have clearly exhibited the powerful efficiency of the ELV nonintrusive method for investigating nonsteady flow problems, such as the transition, separation, and reattachment phenomena on the moving surface.

Experimental Setup and Measurement Procedure

Experiments have been conducted at the Laboratoire Aérodynamique Subsonique Institutionnaire in the S2-Luminy subsonic wind tunnel (rectangular cross section, $0.5 \times 1.0 \text{ m}^2$; length, 3 m; velocity, $U_\infty \leq 20 \text{ m s}^{-1}$) by means of an oscillating device located under the wind-tunnel test section⁴ allowing different kinds of model motions: fore-and-aft, plunging, pitching, and fore-and-aft coupled to pitching.

The airfoil has 30 cm in chord, 49.5 cm in span, and 3.6 cm in thickness (see Fig. 1). No end plates were used, as it has already been shown that the flow is two-dimensional in the middle part of the model,³ where all measurements have been performed. The optical head is mounted on a supporting turntable, which is attached to the oscillating frame as shown in Fig. 1. A beam expander increases the focal distance so that the laser beams are focusing at midspan in the boundary layer through a 45-deg mirror. Because the supporting turntable is linked with the oscillating frame, the u and v velocity components are measured in the reference frame in relative motion. Moreover, the optical head is also installed on a two-dimensional displacement device mounted on the turntable. The measurement volume can then be displaced along the local normal to the surface from $y = 0.2$ to 145 mm with a displacement accuracy of 0.1 mm (Refs. 3 and 4).

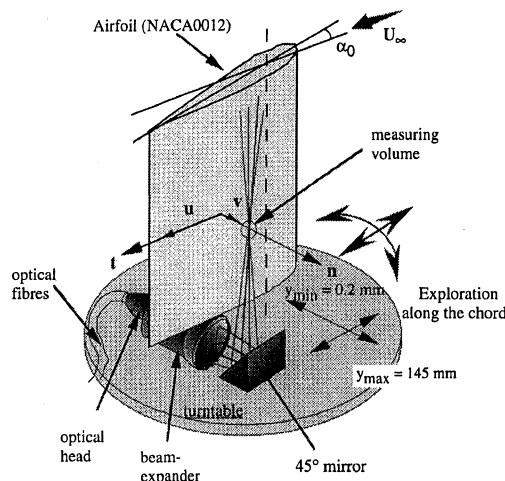


Fig. 1 Embedded measurements linked with oscillating frame model.

The main characteristics of such a two-dimensional ELV system operating in the back scatter mode are as follows. On the blue color, the measurement volume is $0.23 \times 0.23 \times 5.74 \text{ mm}^3$ and the interfringe is $i = 6.10 \text{ mm}$. On the green color, the measurement volume is $0.24 \times 0.24 \times 6.08 \text{ mm}^3$ and the interfringe is $i = 6.44 \text{ mm}$.

Data acquisition is made on a microcomputer from two burst spectrum analyzers delivering for each velocity component (u , v) the Doppler frequencies and the arrival validation time for each frequency measurement. The arrival validation times are counted from a time origin delivered by a photoelectric cell mounted on the oscillating device and providing the airfoil position at each phase of the oscillation. The unsteady data reduction technique is made by using an ensemble average procedure suited for periodic flow investigation, with an accuracy estimated at 4% for the u measurement and 6% for v (Refs. 1 and 3).

Concerning the seeding of the flow, rates of data validation of about 500 Hz are obtained by using a mixture of alcohol and glycerin. The freestream flow is seeded by means of a streamlined tube located in the suction chamber of the wind tunnel.

Transition Phenomenon

As for the steady flow case at $\alpha_0 = 6$ deg, where transition occurs at $s/c = 0.45$ for $Re = 10^5$, the boundary-layer transition in pitching motion is also shown to occur by means of a laminar-separated bubble generated by the strong pressure gradient due to the airfoil curvature. The occurrence of the unsteady transition bubble can be observed from the multicycle acquisition plots of u obtained at different values of k . These plots exhibit no particles validated within a fraction of the period corresponding to the presence of the bubble. Transition occurs just downstream of the bubble. Moreover, at $k = 0.289$, data have been obtained within the bubble showing a negative velocity value area, indicating a mixing process between the bubble and the flow directly to its contact. Other results obtained on U , V , σ_u and δ_1 , δ_2 , δ_3 , H have clearly shown that the transitional and laminarization processes are significantly delayed in time as k increases.⁴

The transition criterion established in previous works^{1,2} on a flat-plate model oscillating either in pitch or in fore-and-aft motion has been applied to the present airfoil in both steady flow and pitching motion.^{3,4} This criterion is based on the integral energy thickness parameter δ_3^* , and is formulated in the form

$$R_{\delta_3^*} = 0.0135 \{1 + 1.5 \exp[-(Re_s/35,000)]\} Re_s^{0.8} \quad (1)$$

with

$$R_{\delta_3^*} = U_e \delta_3^* / \nu \quad \text{and} \quad Re_s = U_e s / \nu \quad (2)$$

The transition criterion is well verified if $R_{\delta_3^*} > R_{\delta_3^*}^*$, with $Re < 3.5 \times 10^5$.

As an example, the efficiency of the above criterion in pitching airfoil is shown in Fig. 2. The boundary-layer survey is performed in this case at $s/c = 0.45$. The experimental values clearly indicate that the transition criterion accurately delimits the laminar regime (open symbols) from the transitional/turbulent regime (solid symbols).

Separation/Reattachment Process

The instantaneous u and v velocity components obtained for different values of k at $s/c = 0.50$, when $\alpha(t) = 9 + 6 \text{ deg} \cos \omega t$,

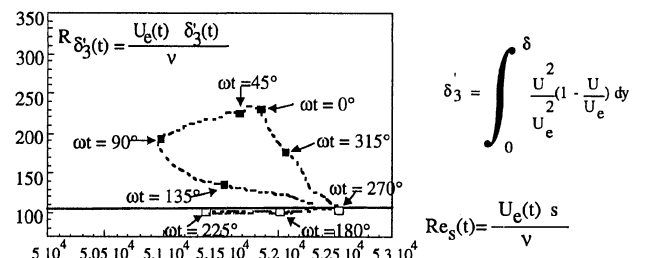


Fig. 2 Transition criterion in pitching motion: $\alpha_0 = 6$ deg, $\Delta\alpha = 2$ deg, and $k = 0.283$. ---, experiment (\square , laminar profiles and \blacksquare , transitional or turbulent profiles); —, transition criterion: $R_{\delta_3^*}^* = 0.0135 \{1 + 1.5 \exp[-(Re_s/35,000)]\} Re_s^{0.8}$.

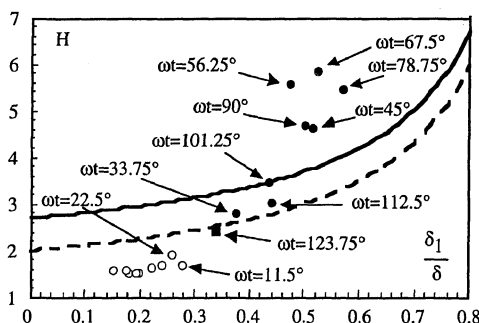


Fig. 3 Separation criterion in pitching motion. Sandborn and Kline's⁵ criterion: —, fully developed separation and ---, intermittent separation. Experiments: ○, attached flow: 0 deg < ωt < 22.5 deg; ωt = 135 deg; 281.25 deg < ωt < 360 deg; ■, intermittent reattachment: ωt = 123.75 deg; and ●, fully developed separation: 33.75 deg < ωt < 123.75 deg.

have clearly pointed out that the transition, the separation, and the reattachment process are delayed as k increases. Moreover, it is possible to determine all along the period the nature of the boundary layer (attached, separated, near separation, or reattachment) by analyzing the simultaneous evolution of the u tangential profile and turbulence intensity σ_u obtained by the ELV method.⁴

From such results, it can also be concluded that the duration of the separation along the oscillation period is shown to decrease when the reduced frequency k increases.

In steady flow regimes, the Sandborn and Kline's⁵ criterion is based on the shape factor H , which is expressed as a function of δ_1/δ ,

$$H_{\text{sep}} = A + \left[\frac{1}{1 - (\delta_1/\delta)} \right] \quad (3)$$

Such a criterion, which appears also to be able to differentiate intermittent separations ($A = 1$) (for more than 5% of the time the flow moves upstream, $u < 0$) from fully developed separations ($A = 1.70$) (for more than 50% of the time the flow moves upstream, $u < 0$), has been applied successfully to characterize the boundary-layer separation on the airfoil in steady flow configurations. Moreover, this steady flow configuration study has shown that the reattachment process is also affected by the intermittency phenomenon.⁴

Because of the similarity observed on the (U , V , σ_u) profiles during the separation process occurring on the NACA 0012 airfoil in either steady flow or pitching motion,⁶ an attempt to check the Sandborn and Kline's⁵ separation criterion has been made in this study. An example of an application of this criterion is shown in Fig. 3 for the pitching motion case corresponding to $k = 0.283$. The Sandborn and Kline criterion appears to be well suited to delimiting the attached boundary-layer regime (open symbols) and the separated flow regimes (solid symbols) in the unsteady flow generated by the pitching motion. However, within the separated zone the criterion appears to be less efficient in differentiating the intermittent separation from the fully developed separation. In Fig. 3, the fully developed separation is identified by the criterion as an intermittent type separation at $\omega t = 33.75$ deg.

Conclusion

In the present study, the ELV method has been successfully extended to two-dimensional velocity measurements (u , v) around moving curved walls and airfoils oscillating in pitching motion.

The transition criterion previously established on an oscillating flat-plate model is also shown to be valid on the NACA 0012 airfoil either in steady flow or in pitching motion, at least under our experimental conditions.

Concerning the separation/reattachment process, the Sandborn and Kline criterion appears to be well suited to delimiting attached and separated flow regimes. A refinement of this criterion seems to be required for differentiating intermittent and fully separated regimes. Moreover, the cyclic separation/reattachment process is shown to be strongly influenced by the reduced frequency parameter k .

The increase of the frequency k is shown to produce a time delay on the transition, separation, and reattachment processes.

Acknowledgments

The authors are thankful for the support provided by the "Direction des Recherches, Etudes et Techniques" under Grants 87/272 and 91/158.

References

- ¹Favier, D., Maresca, C., Renon, P., and Autric, J. M., "Boundary-Layer Measurements on Oscillating Models Using an Optical Fibre LDA Technique," *Proceedings of the Sixth International Symposium on Applications of Laser Techniques to Fluid Mechanics*, Durao Edit., Lisbon, Portugal, 1992, pp. 1341-1346.
- ²Pascasio, M., Autric, J. M., Favier, D., and Maresca, C., "Etude de la Couche Limite sur une Plaque Plane Oscillant en Tangage par Vélocimétrie Laser Embarquée," *Proceedings of the Eleventh French Congress of Mechanics*, Dymont Edit., Lille, France, 1993, pp. 253-257.
- ³Favier, D., Maresca, C., and Pascasio, M., "Etude Expérimentale et Numérique du Décollement de la Couche Limite Instationnaire sur un Modèle Oscillant en Ecoulement 2D/3D," *Direction des Recherches Etudes et Techniques*, Contract 91/158, Synthesis Rept., Paris, Oct. 1994.
- ⁴Pascasio, M., "Contribution Expérimentale et Numérique de la Couche Limite se Développant sur un Profil d'Aile Oscillant: Phénomènes de Transition et de Décollement en Ecoulement Instationnaire," Ph.D. Thesis, Dept. of Mechanics, Univ. of Aix, Marseille II, France, 1995.
- ⁵Sandborn, V. A., and Kline, S. J., "Flow Models in Boundary Layer Stall Conception," *Journal of Basic Engineering*, 1961, pp. 317-327.
- ⁶Pascasio, M., Autric, J. M., Favier, D., and Maresca, C., "Unsteady Boundary-Layer Measurement on Oscillating Airfoils: Transition and Separation Phenomena in Pitching Motion," *Proceedings of the AIAA 34th Aerospace Sciences Meeting* (Reno, NV), AIAA, Washington, DC, 1996 (AIAA Paper 96-0035).

Numerical Simulation of Vortex-Induced Oblique Shock-Wave Distortion

Donald P. Rizzetta*

U.S. Air Force Wright Laboratory,
Wright-Patterson Air Force Base, Ohio 45433-7913

Introduction

INTERSECTIONS between streamwise vortices and oblique shock waves occur in a number of practical situations and commonly result in complex three-dimensional flowfields. These events typically involve vortices that are produced by the fore bodies and lifting surfaces of supersonic vehicles or by the tips of canards, fins, and wings. Such vortices then interact with the associated shock-wave systems present over wings or control surfaces, or within high-speed inlets, and may result in loss of lift, increased drag, adverse stability and control, or decreased engine performance. When the interactions are sufficiently strong, vortex breakdown can be induced.

Previous experimental and numerical investigations of shock-wave/vortex interactions are reviewed in Ref. 1. Of these, only the computations of Rizzetta² attempted to provide a direct comparison between numerical calculations and experimental data. It was indicated that although solutions to the Euler equations compared reasonably well with measurements in a number of cases, they could not reproduce the vortex breakdown that was often observed experimentally. The purpose of the present work is to simulate oblique shock-wave/wing-tip vortex interactions via solution to the compressible three-dimensional mass-averaged turbulent

Received Dec. 27, 1995; presented as Paper 96-0039 at the AIAA 34th Aerospace Sciences Meeting, Reno, NV, Jan. 15-18, 1996; revision received Oct. 1, 1996; accepted for publication Oct. 4, 1996; also published in *AIAA Journal on Disc*, Volume 2, Number 2. This paper is declared a work of the U.S. Government and is not subject to copyright protection in the United States.

*Research Aerospace Engineer, Computational Fluid Dynamics Research Branch, Aeromechanics Division, Associate Fellow AIAA.